11

Dense nuclear matter

One aspect of nuclear physics is the study of nuclear matter. Up until the mid 1970s, nearly all studies used a nonrelativistic potential to describe the nucleon–nucleon interaction. The results were not entirely satisfactory. It was difficult to obtain simultaneously the saturation density (about 0.153 nucleons per fm^3) and the binding energy (about 16.3 MeV per nucleon with the Coulomb force turned off) in a microscopic nonrelativistic approach. Part of the discrepancy was ascribed to three-body interactions. However, relativity can also play a small but significant role at normal nuclear matter density. The importance of relativity may be judged by comparing the Fermi momentum p_F with the nucleon mass. The baryon density is

$$n = \frac{2p_\mathrm{F}^3}{3\pi^2} \tag{11.1}$$

At normal nuclear density $p_\mathrm{F} = 259$ MeV, and at four times normal nuclear density $p_\mathrm{F} = 411$ MeV. These should be compared with the vacuum nucleon mass $m_N = 939$ MeV and the Fermi kinetic energy

$$K_\mathrm{F} = m_N \left[(1 - v_\mathrm{F}^2)^{-1/2} - 1\right] = \tfrac{1}{2}m_N v_\mathrm{F}^2 + \tfrac{3}{8}m_N v_\mathrm{F}^4 + \cdots \tag{11.2}$$

Although one might think that the relativistic correction at normal nuclear density, which is of order v_F^4 and numerically about 2 MeV, is rather small, still it is not insignificant compared with the binding energy of 16.3 MeV. Of course, at higher densities, relativity certainly cannot be ignored. As we shall learn, relativity plays an even greater role in the interactions among nucleons. The relativistic approach to nuclear matter was pioneered by Johnson and Teller [1], Duerr [2], and Walecka [3].
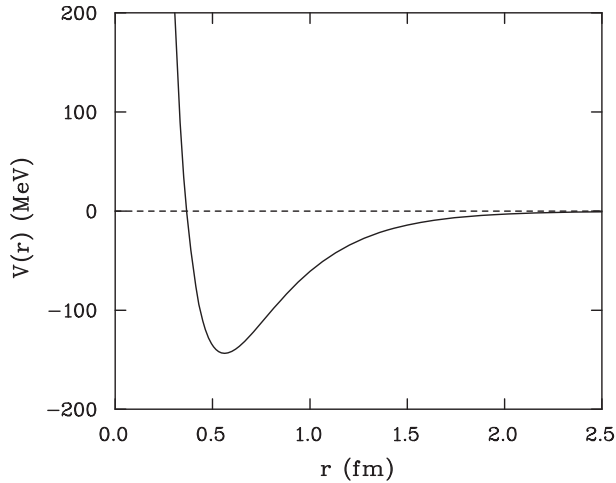
Fig. 11.1.   Model of the nucleon–nucleon potential illustrating long-range attraction and short-range repulsion. The parameters are given in the text.

11.1 Walecka model

The force between nucleons is conventionally thought of as mediated by the exchange of mesons. The long-range part of the nuclear force comes from one-pion exchange. Its range is $1/m_\pi = 1.4$ fm. However, this averages to zero unless parity is broken. The force mediated by exchange of the ρ meson vanishes in isospin-symmetric matter (equal numbers of protons and neutrons); the dominant one-meson exchanges in isospin-symmetric nuclear matter come from the omega meson (ω) and a scalar meson (σ). The ω is a vector meson, is electrically neutral, and has a mass of about 783 MeV. The σ meson represents a very broad resonance in $\pi\pi$ scattering at 500–600 MeV. The exchange of the electrically neutral σ is usually thought of as simulating some part of two-pion exchange. With single-ω and single-σ exchange, the static nonrelativistic potential between two nucleons is the sum of two Yukawa interactions:

$$V(r) = \frac{g_\omega^2}{4\pi} \frac{e^{-m_\omega r}}{r} - \frac{g_\sigma^2}{4\pi} \frac{e^{-m_\sigma r}}{r} \tag{11.3}$$

If $g_\omega > g_\sigma$ and $m_\omega > m_\sigma$ then the potential looks like that shown in Figure 11.1. It is attractive at long distances and repulsive at short distances and so has the structure necessary to bind nuclear matter.

The Lagrangian that contains the Yukawa couplings of the nucleon to the ω and to the σ is

$$\begin{aligned}
\mathcal{L}_W = {}& \bar{\psi}(i\,\partial\!\!\!/ - m_N + g_\sigma\sigma - g_\omega\,\omega\!\!\!/)\psi \\
& + \tfrac{1}{2}\left(\partial_\mu\sigma\partial^\mu\sigma - m_\sigma^2\sigma^2\right) - \tfrac{1}{4}F^{\mu\nu}F_{\mu\nu} + \tfrac{1}{2}m_\omega^2\omega_\mu\omega^\mu
\end{aligned} \tag{11.4}$$

where

$$F_{\mu\nu} = \partial_\mu \omega_\nu - \partial_\nu \omega_\mu$$

Now of course we know that baryons and mesons are not elementary point particles. They are composite structures of quarks and gluons. The idea of an effective-nuclear-field theory is to write down a Lagrangian that contains the low-lying baryons and mesons as relativistic fields. This allows us to use the standard machinery of relativity, quantum mechanics, and statistical mechanics. This approach will break down if we attempt to probe the theory at very short distances, say a few tenths of a fermi, since then the quarks and gluons must manifest themselves.

Let us investigate the properties of dense nuclear matter using the Lagrangian $\mathcal{L}_W$. The partition function is

$$Z = \int \left[d\bar{\psi}_p \right] \left[d\psi_p \right] \left[d\bar{\psi}_n \right] \left[d\psi_n \right] \left[d\sigma \right] \left[d\omega_\mu \right]$$
$$\times \exp \left(\int_0^\beta d\tau \int d^{3x} \left(\mathcal{L}_W + \mu_p \psi_p^\dagger \psi_p + \mu_n \psi_n^\dagger \psi_n \right) \right) \quad (11.5)$$

where μ_p and μ_n are the proton and neutron chemical potentials. For isospin-symmetric matter $\mu_p = \mu_n$ and for pure neutron matter $\mu_p = 0$, $\mu_n \neq 0$ (although the presence of electrons in a neutron star allows $\mu_p \neq 0$). For the remainder of this section, we concentrate on symmetric matter and write $\mu = \mu_n = \mu_p$.

The nucleons act as sources in the meson field equations. This suggests that a net baryon density will generate scalar and vector meson condensates. This can be checked by allowing σ and ω_μ to have nonzero expectation values. Thus we write

$$\sigma = \bar{\sigma} + \sigma'$$
$$\omega_\mu = \delta_{\mu 0} \bar{\omega}_0 + \omega'_\mu \quad (11.6)$$

where the bar indicates the ensemble average value of the field and the prime indicates the fluctuation about the average. (Note that $\bar{\omega}_i = 0$ on account of rotational symmetry.) In the *mean field approximation*, one neglects fluctuations in the meson fields. This means that the nucleons are taken to move independently in the mean fields $\bar{\sigma}$ and $\bar{\omega}_0$, which themselves are generated self-consistently by the nucleons. Based on the success of the nuclear shell model, we anticipate that this will provide a reasonable first-order estimate of the properties of dense nuclear matter. The Lagrangian $\mathcal{L}_W$ is commonly referred to as the Walecka Lagrangian, and when used in conjunction with the mean field approximation is referred to as the Walecka model.

The partition function may be evaluated exactly in the mean field approximation because the functional integral is just a product of Gaussian integrals. The argument of the exponential in (11.5) is thus approximated by

$$\bar{\psi}\left[i\,\partial\!\!\!/ - (m_N - g_\sigma\bar{\sigma}) + (\mu - g_\omega\bar{\omega}_0)\gamma_0\right]\psi - \tfrac{1}{2}m_\sigma^2\bar{\sigma}^2 + \tfrac{1}{2}m_\omega^2\bar{\omega}_0^2 \qquad (11.7)$$

This means that the nucleon develops an effective mass

$$m_N^* = m_N - g_\sigma\bar{\sigma} \qquad (11.8)$$

and an effective chemical potential

$$\mu^* = \mu - g_\omega\bar{\omega}_0 \qquad (11.9)$$

Using (11.5) together with (11.7), we obtain the pressure as

$$P(\mu, T) = P_{\text{FG}}(\mu^*, T) - \tfrac{1}{2}m_\sigma^2\bar{\sigma}^2 + \tfrac{1}{2}m_\omega^2\bar{\omega}_0^2 \qquad (11.10)$$

where P_{FG} is the Fermi-gas expression for nucleons with the quoted effective mass and chemical potential.

We now must determine the mean fields $\bar{\sigma}$ and $\bar{\omega}_0$. If we allow $\bar{\sigma}$ and $\bar{\omega}_0$ to vary, the equilibrium configuration will be attained when P is an extremum. Thus

$$\bar{\sigma} = -\left(\frac{g_\sigma}{m_\sigma^2}\right)\frac{\partial P_{\text{FG}}}{\partial m_N^*} \qquad (11.11)$$

$$\bar{\omega}_0 = \left(\frac{g_\omega}{m_\omega^2}\right)\frac{\partial P_{\text{FG}}}{\partial \mu^*} \qquad (11.12)$$

Of these, the vector condensate can be determined directly in terms of the baryon density n:

$$\bar{\omega}_0 = \frac{g_\omega}{m_\omega^2}n \qquad (11.13)$$

A quick calculation utilizing (2.99) shows that the scalar condensate is proportional to the scalar density n_s:

$$\bar{\sigma} = \frac{g_\sigma}{m_\sigma^2}n_s \qquad (11.14)$$

where

$$n_s \equiv 4\int\frac{d^3p}{(2\pi)^3}\frac{m_N^*}{E^*}\left(\frac{1}{e^{\beta(E^*-\mu^*)}+1}+\frac{1}{e^{\beta(E^*+\mu^*)}+1}\right)$$
$$E^* = \sqrt{p^2 + m_N^{*2}}$$

$$(11.15)$$

Equation (11.14) is a self-consistent equation to be solved for m_N^*, as may be seen from the alternate form

$$m_N^* = m_N - \left(\frac{g_\sigma^2}{m_\sigma^2}\right) n_{\mathrm{s}} \tag{11.16}$$

Now let us focus on cold nuclear matter and delay the discussion of finite temperature to a later section. Using the above equations and the standard thermodynamic identities, we have

$$P = \frac{1}{4\pi^2} \left[\frac{2}{3} E_{\mathrm{F}}^* p_{\mathrm{F}}^3 - m_N^{*2} E_{\mathrm{F}}^* p_{\mathrm{F}} + m_N^{*4} \ln\left(\frac{E_{\mathrm{F}}^* + p_{\mathrm{F}}}{m_N^*}\right)\right]$$
$$+ \frac{1}{2}\left(\frac{g_\omega^2}{m_\omega^2}\right) n^2 - \frac{1}{2}\left(\frac{g_\sigma^2}{m_\sigma^2}\right) n_{\mathrm{s}}^2 \tag{11.17}$$

$$\epsilon = \frac{1}{4\pi^2} \left[2 E_{\mathrm{F}}^{*3} p_{\mathrm{F}} - m_N^{*2} E_{\mathrm{F}}^* p_{\mathrm{F}} - m_N^{*4} \ln\left(\frac{E_{\mathrm{F}}^* + p_{\mathrm{F}}}{m_N^*}\right)\right]$$
$$+ \frac{1}{2}\left(\frac{g_\omega^2}{m_\omega^2}\right) n^2 + \frac{1}{2}\left(\frac{g_\sigma^2}{m_\sigma^2}\right) n_{\mathrm{s}}^2$$

where

$$n = \frac{2}{3\pi^2} p_{\mathrm{F}}^3$$

$$E_{\mathrm{F}}^* = \mu^* = \sqrt{p_{\mathrm{F}}^2 + m_N^{*2}}$$

$$m_N^* = m_N - \left(\frac{g_\sigma^2}{m_\sigma^2}\right) n_{\mathrm{s}}$$

$$n_{\mathrm{s}} = \frac{m_N^*}{\pi^2} \left[E_{\mathrm{F}} p_{\mathrm{F}} - m_N^{*2} \ln\left(\frac{E_{\mathrm{F}}^* + p_{\mathrm{F}}}{m_N^*}\right)\right]$$

In these equations it is natural to take the Fermi momentum p_{F} as the one independent variable. Notice that this equation of state is given essentially in analytic form with only the equation for m_N^* to be solved self-consistently.

Before investigating the equation of state in detail, it is worthwhile to consider the extremes of low and high density. At low density $p_{\mathrm{F}} \to 0$, and we recover the equation of state of a nonrelativistic ideal Fermi gas.

The quantities in (11.17) have the following limits:

$$P \to \frac{2}{15\pi^2} \frac{p_F^5}{m_N}$$

$$\epsilon \to \left(m_N + \frac{3}{10} \frac{p_F^2}{m_N} \right) n \qquad (11.18)$$

$$m_N^* \to m_N$$

$$n_s \to n$$

At high density, $p_F \to \infty$, the effective nucleon mass goes to zero:

$$m_N^* \to \frac{m_N}{1 + (g_\sigma^2/\pi^2)(p_F^2/m_\sigma^2)} \qquad (11.19)$$

The pressure and energy density are dominated by the vector mean field:

$$P \to \epsilon \to \frac{1}{2} \left(\frac{g_\omega^2}{m_\omega^2} \right) n^2 \qquad (11.20)$$

Thus the speed of sound, $c_s^2 = \partial P/\partial \epsilon$, approaches the speed of light at very high density. This is to be compared with the speed in sound in a massless Fermi gas, which is $1/\sqrt{3}$.

In these equations there are only two parameters at our disposal, g_ω^2/m_ω^2 and g_σ^2/m_σ^2. The nucleon mass is $m_N = 939$ MeV and the vector meson mass is $m_\omega = 783$ MeV. For definiteness we take $m_\sigma = 550$ MeV, corresponding to the scalar–isoscalar resonance in $\pi-\pi$ scattering. Then the choice of couplings $g_\omega^2/4\pi = 14.717$ and $g_\sigma^2/4\pi = 9.537$ leads to a binding energy of 16.3 MeV per nucleon and a saturation density of 0.153 nucleons per fm^3. The curve of energy per nucleon versus density is shown in Figure 11.2. The energy per nucleon rises rather dramatically with density. In fact the compressibility of nuclear matter at saturation density turns out to be

$$K \equiv p_F^2 \frac{d^2(\epsilon/n)}{dp_F^2} = 563 \text{ MeV} \qquad (11.21)$$

The generally accepted value, based on measurements of the isoscalar giant monopole resonance in heavy nuclei, is 250 ± 30 MeV [4–7]. The Walecka model predicts $m_N^* = 0.57 m_N$, which is somewhat smaller than some estimated values of the effective nucleon mass at nuclear saturation density [8] but quite consistent with others [9, 10]. Nevertheless, we should not expect to fit a large body of nuclear-matter properties to high accuracy for several reasons: (i) the Lagrangian $\mathcal{L}_W$ is too simple to represent accurately the complicated nuclear forces, and (ii) the mean field approximation neglects nucleon–nucleon correlations.
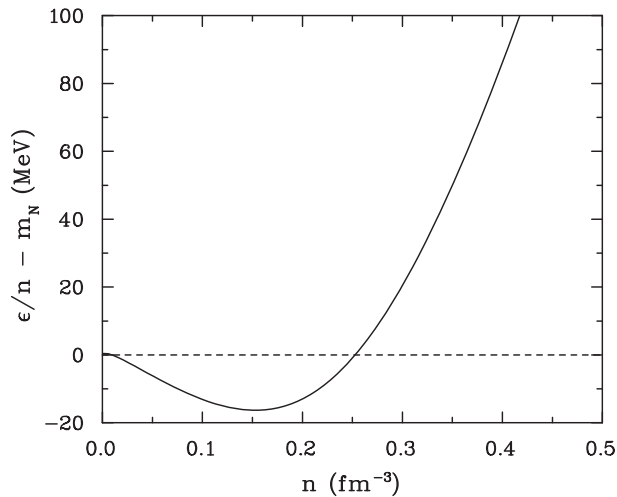
Fig. 11.2. The average energy per nucleon minus the nucleon mass as a function of the baryon density in the mean field approximation to the Walecka model.

One may ask whether the numerical values obtained for the two Yukawa couplings are reasonable. Fitting nucleon–nucleon phase shifts up to 300 MeV typically yields similar values. For example, Machleidt, Holinde, and Elstor [11] used a boson-exchange model employing the π, ρ, ω, and σ mesons, and found that $g_\omega^2/4\pi = 20$ and $g_\sigma^2/4\pi = 9.2$. This agreement is satisfactory considering that the Yukawa couplings used in the mean field approach are really effective couplings that are fine-tuned to mimic all the many-body effects not included. Fine-tuning is actually required in the Walecka model, where the delicate cancelation between short-range vector repulsion and medium-range scalar attraction is really a relativistic effect. This may be seen in the following way. In the nonrelativistic mean field approximation the average potential energy felt by a nucleon is

$$\langle V \rangle = n \int d^3r\, V(r) \qquad (11.22)$$

The average kinetic energy is $(3/5)(p_F^2/2m_N)$. Since $n \propto p_F^3$ this means that $\int d^3r\, V(r) > 0$ for the energy to be bounded from below. Hence both the average kinetic and potential energies must be positive at all densities, and an equilibrium bound state cannot arise. Relativity plays an important role in the sense that the baryon (vector) density and the scalar density are not the same; they differ by a velocity factor m_N^*/E^* in the relevant integrands at zero temperature. In this vein it is illustrative to expand the energy per nucleon as a power series in the Fermi velocity at $T = 0$. The difference between the scalar and baryon densities shows
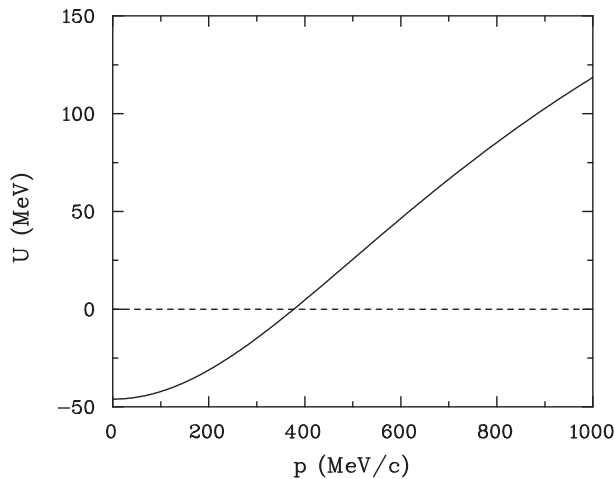
Fig. 11.3.   The nuclear optical potential as a function of momentum at nuclear saturation density in the Walecka model.

up at order v_{F}^5, which is just one power more than the first relativistic correction to the kinetic energy. See, for example, Serot and Walecka [12].

   The nuclear optical potential U is defined by

$$E(p, p_{\mathrm{F}}) = \sqrt{p^2 + m_N^2} + \mathrm{U}(p, p_{\mathrm{F}}) \tag{11.23}$$

Here E is the single-particle energy of a nucleon. The optical potential is both density and momentum dependent. From (11.10), (11.14), and (11.16),

$$E(p, p_{\mathrm{F}}) = \sqrt{p^2 + m_N^{*2}} + \left(\frac{g_\omega^2}{m_\omega^2} \right) n \tag{11.24}$$

The optical potential at saturation density is plotted in Figure 11.3. Various phenomenological optical potentials of this form are widely used in interpreting proton–nucleus scattering [13] and nucleus–nucleus scattering [14, 15] at energies of several hundred MeV. The optical potential in the Walecka model rises too rapidly at high momentum compared with the data. Such disagreement should not be a surprise, for the reasons given above.

11.2 Loop corrections

The mean field used in the previous section has two great advantages: it is relativistically and thermodynamically self-consistent, neither of which is a trivial achievement. By fine-tuning only two input parameters, the binding energy and the density of cold isospin-symmetric nuclear matter, one

may extrapolate to both lower and higher densities, to isospin-asymmetric matter (after the ρ meson is included, see Chapter 16), and to moderate temperatures. However, the coupling constants are large, of the order of 10, making a convergent loop expansion highly unlikely. Both one-loop and two-loop corrections have been computed in the Walecka model, and we shall present the results in this section. The two-loop corrections, in particular, are very large, as expected. However, nucleons are composite objects, constructed from quarks and gluons. Therefore any effective theory using baryons and mesons as the degrees of freedom will necessarily bring form factors into play. It will turn out that with reasonable choices of the form factors, the sum of the two-loop contributions to the energy per nucleon is surprisingly small. This does not, of course, imply that other physical observables are also small.

11.2.1 Relativistic Hartree

The Walecka model is renormalizable even though it has a massive vector boson because it couples to the conserved baryon current. Regarding the scalar boson, the Walecka model truncates the Lagrangian at order σ^2. However, all terms that keep the theory renormalizable and respect the symmetries can and should be kept. This means powers of σ up to and including 4. In fact, these are required in order to cancel divergences coming from the shift in the zero-point energy of the nucleons. Relative to the vacuum, the shift in the zero-point energy is [16]

$$\epsilon_{\text{ZP}}(m_N^*) = -2 \int \frac{d^3p}{(2\pi)^3} \left(\sqrt{p^2 + m_N^{*2}} - \sqrt{p^2 + m_N^2} \right) - \sum_{n=1}^{4} \frac{c_n}{n!} \sigma^n \tag{11.25}$$

The coefficients c_n of the counterterms are dependent upon the regularization scheme. In momentum-cutoff schemes they diverge as the cutoff goes to infinity, and in dimensional regularization schemes they diverge as four dimensions are approached. The minimal procedure is to choose the c_n so as to cancel the first four powers of σ arising from the integration over momentum. (Recall that $m_N^* = m_N - g_\sigma \bar{\sigma}$.) Although this procedure is not unique, it has the feature of minimizing the many-body forces arising from this vacuum correction. The result is

$$\epsilon_{\text{ZP}}(m_N^*) = -\frac{1}{4\pi^2} \left[m_N^{*4} \ln \left(\frac{m_N^*}{m_N} \right) + m_N^3(m_N - m_N^*) - \frac{7}{2} m_N^2 (m_N - m_N^*)^2 \right.$$
$$\left. + \frac{13}{3} m_N(m_N - m_N^*)^3 - \frac{25}{12} (m_N - m_N^*)^4 \right] \tag{11.26}$$

This formula assumes an isospin degeneracy factor 2.

The pressure and energy density in the one-loop relativistic Hartree approximation are related to those in the relativistic mean field

approximation by

$$P_{\mathrm{RH}} = P_{\mathrm{MF}} - \epsilon_{\mathrm{ZP}}$$
$$\epsilon_{\mathrm{RH}} = \epsilon_{\mathrm{MF}} + \epsilon_{\mathrm{ZP}} \tag{11.27}$$

This equation of state is also thermodynamically consistent. Minimizing the energy at fixed density leads to a modification of the mean field self-consistency condition for the scalar condensate, namely

$$m_N^* = m_N - \left(\frac{g_\sigma^2}{m_\sigma^2}\right) n_{\mathrm{s}} + \frac{g_\sigma^2}{m_\sigma^2} \frac{1}{\pi^2} \left[m_N^{*3} \ln\left(\frac{m_N^*}{m_N}\right) - m_N^2 (m_N - m_N^*) \right.$$
$$\left. - \frac{5}{2} m_N (m_N - m_N^*)^2 - \frac{11}{6} (m_N - m_N^*)^3 \right] \tag{11.28}$$

A small change to the parameters in (11.4) again reproduces the saturation density and binding energy of nuclear matter. Numerical results will be shown in the next subsection, where we consider two-loop contributions.

11.2.2 Two loops

Two-loop contributions to the partition function can be performed in the usual fashion. The general form is

$$\ln Z_2 = -\frac{1}{2} \sum_{n_1 n_2} \int \frac{d^3 p_1}{(2\pi)^3} \frac{d^3 p_2}{(2\pi)^3} \mathrm{Tr}\left[\mathcal{G}(p_1)\Gamma(p_1,p_2,k)\ \mathcal{G}(p_2)\Gamma(p_2,p_1,k)\mathcal{D}(k) \right]$$

$$\tag{11.29}$$

Here $\mathcal{G}$ is the nucleon propagator, $\mathcal{D}$ is the boson propagator (for either the scalar or vector meson), Γ is the relevant vertex, and $k = p_1 - p_2$. Lorentz and Dirac indices are suppressed.

These contributions have been evaluated at zero temperature by Furnstahl, Perry, and Serot [17]. The two-loop diagram has several physical contributions. One contribution originates from the exchange of momentum between two nucleons in the Fermi sea. A second contribution comes from the Lamb shift, the change in the properties of a nucleon as it propagates in the medium. The third contribution is a shift in the zero-point vacuum fluctuations owing to the presence of nuclear matter. Unfortunately the results cannot be expressed in terms of elementary functions because the nucleon and meson masses are all nonzero. The diagrams are as follows:
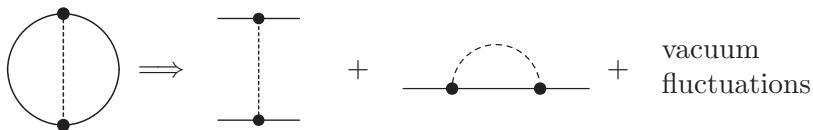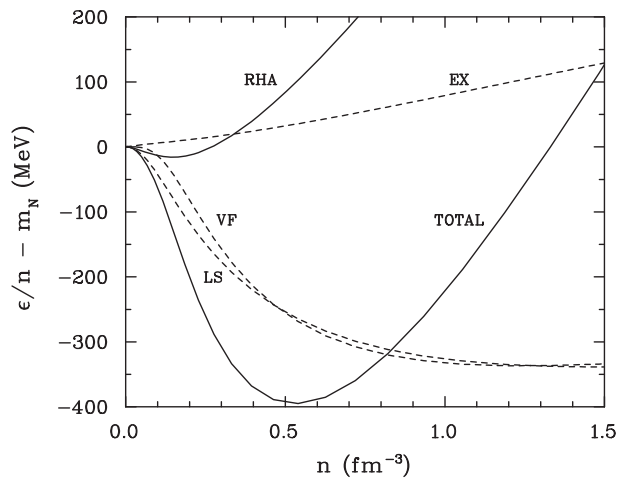
Fig. 11.4. The energy per nucleon as a function of density. The solid curve labeled RHA is the relativistic Hartree approximation. The solid curve labeled TOTAL includes the exchange, Lamb shift, and two-loop vacuum fluctuations as well. Point vertices are used.

Figure 11.4 shows the equation of state in the relativistic Hartree approximation (RHA). In this figure the values of the parameters are $g_\sigma^2/4\pi = 4.32$, $m_\sigma = 458$ MeV, $g_\omega^2/4\pi = 8.18$, and $m_\omega = 783$ MeV. Also shown are the contributions from the exchange term, the Lamb shift, and the vacuum fluctuations. They are computed as if they were perturbations, with no change in the numerical values of the coupling constants. The exchange term is relatively modest but the Lamb shift and the vacuum fluctuations are enormous. When all are added, the binding energy changes to nearly 400 MeV from 16 MeV at a density of 3.7 times the empirical value. The two-loop contributions are not perturbatively small, quite the contrary. This is not unexpected, owing to the large values of the coupling constants. Undoubtedly higher-loop contributions are important too, and the whole calculational scheme breaks down.

11.2.3 Form factors

The integrals in the two-loop terms receive contributions from internal momenta as high as 5 GeV. But nucleons and mesons are not point particles. Their finite spatial size should soften these contributions significantly. Prakash, Ellis, and Kapusta [18] introduced form factors at both vertices with the philosophy that they do not arise from interactions within the confines of the Walecka model. The origin of these form factors runs deeper, back to the quark and gluon substructure of hadrons. Of course, the full meson–nucleon vertex function will include dressings

from the hadronic degrees of freedom too. A consistent treatment of form factors is not yet available. In general, they will involve several scalar functions, the number of which depends on the Lorentz structure of the vertex. Each one may depend on the invariants p_1^2, p_2^2, and k^2. The minimal assumption is that the scalar and vector form factors are functions of k^2 only and have the simple monopole form

$$f(k^2) = \frac{1}{1 - k^2/\Lambda^2} \tag{11.30}$$

when $k^2 < 0$ (spacelike) and where Λ is a cutoff of order 1 GeV. Then the vertices to be used in the two loop diagrams are just the point vertices multiplied by $f(k^2)$.

Three comments are in order. First, the selection of relativistic monopole form factors with a cutoff of this order is consistent with the relativistic dipole structure of the on-shell nucleon electromagnetic form factor. In that case, one monopole factor arises from the finite size of the nucleon while the other arises from the ρ meson propagator in the context of the vector-meson-dominance model [19]. Second, if one were to include the off-mass-shell p_1^2 and p_2^2 dependences as well then it might be possible to get an even greater suppression of the two-loop contributions than that displayed in Figure 11.5. Third, since the vector meson couples to the baryon current there is a generalized type of Ward identity. This identity is different from that in QED because in the strong-interaction case the vector–current coupling is nonlocal. Since the form factor $f(k^2)$ is taken to be intrinsic to the nucleon rather than generated by the Yukawa interactions of the nucleons with the meson fields, there is no inconsistency in using the mean field propagators in the loop expansion. To lowest order in g_σ and g_ω the identity must be such that it is satisfied by the free-field form of the nucleon and meson propagators.

Multiplying the bare point-particle vertices by $f(k^2)$, it can easily be shown that the energy density is obtained from the identity

$$\epsilon = \frac{\Lambda^2}{\Lambda^2 - m^2} \left\{ \frac{\Lambda^2}{\Lambda^2 - m^2} \left[\epsilon_{\text{pt}}(m^2) - \epsilon_{\text{pt}}(\Lambda^2) \right] + \frac{d\epsilon_{\text{pt}}(\Lambda^2)}{d \ln \Lambda^2} \right\} \tag{11.31}$$

Here m is the mass of the exchanged meson and ϵ_{pt} is the two-loop energy density with point vertices.

Figure 11.5 shows what happens when form factors are inserted at each vertex with the cutoff chosen as 1 GeV for both the scalar and vector meson vertices. There is a tremendous reduction compared with the case of point vertices. Near the equilibrium density, both the scalar and vector meson exchange terms are reduced by 10%–15%. For the Lamb shift the reduction is by a factor 5 for scalar mesons and by a factor 10 for the vector mesons. The vacuum fluctuation contributions are reduced
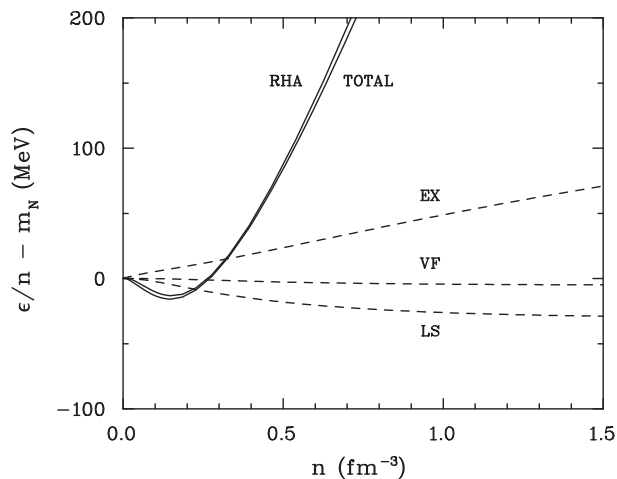
Fig. 11.5. The same as Figure 11.4 except that form factors with $\Lambda = 1$ GeV have been used at each vertex.

by similar amounts. Because the exchange terms are generally positive while the other two are negative in the density range shown in the figure, the final result is a reduction in the two-loop contribution by a factor of more than 100. Now the largest contribution is the exchange, followed by the Lamb shift and vacuum fluctuations. This is satisfying, in the sense that the exchange term survives in the quantum nonrelativistic limit whereas the Lamb shift and vacuum fluctuations are truly field theoretic in origin. With the form factors included, the two-loop contributions really are perturbative additions to the relativistic Hartree equation of state. A minimization of the Hartree equation plus two-loop contributions with respect to the effective nucleon mass at each density gives results nearly identical to those neglecting the two-loop contributions.

As the cutoff Λ increases, the two-loop contributions increase in magnitude, of course. When Λ is increased to 1.5 GeV the binding energy is increased by 11 MeV and the equilibrium density increases by about 30%. A small change in the coupling constants will restore the location of the empirical minimum in the equation of state.

It still remains a great challenge in strong-interaction physics to understand in detail the nature and structure of these form factors. The point of view presented here is that form factors represent the quark and gluon substructure of hadrons and cannot be calculated within the boundaries of hadronic degrees of freedom alone; one unfortunate consequence is that this renders the theory unrenormalizable. This is not the only point of view to which one may subscribe. For example, Serot and Tang [20] computed the effects of vertex corrections within the Walecka model

itself instead of using imposed form factors. Whatever the point of view, however, it seems that the relativistic Hartree approximation, or even the mean field approximation, may not be an unreasonable approach to parametrizing the nuclear equation of state. It is consistent with our empirical knowledge near the equilibrium point and with relativity and the thermodynamic identities.

11.3 Three- and four-body interactions

The Lagrangian given in (11.5) represents a renormalizable theory. Even though a low-energy effective theory need not be renormalizable (form factors should cut off unphysical short distance contributions) one may desire to keep this property. Then one may add the cubic and quartic terms $-\frac{1}{3}bm_N(g_\sigma\sigma)^3 - \frac{1}{4}c(g_\sigma\sigma)^4$ to the Lagrangian. Just as σ^2 represents a two-body interaction, σ^3 represents a three-body interaction (a vertex with three σ lines emanating from it and attached to external nucleon lines) and σ^4 represents a four-body interaction (a vertex with four σ lines emanating from it and attached to external nucleon lines). It has been found that a phenomenological three-body interaction is necessary to describe bound nuclear matter in a nonrelativistic-potential approach. There is less information available on a microscopic four-body interaction.

In the relativistic mean field approach, the cubic and quartic terms can be used to fit more of the empirically known properties of nuclear matter. These include the following:

the saturation density [4]

$$n_0 = 0.153 \text{ fm}^{-3} \tag{11.32}$$

the binding energy [4]

$$\frac{\epsilon}{n} - m_N = -16.3 \text{ MeV} \tag{11.33}$$

the Landau mass [8]

$$m_{\mathrm{L}} = \sqrt{m_N^{*2} + p_{\mathrm{F}}^2} = 0.83 m_N \tag{11.34}$$

the compressibility [4–7]

$$K = p_{\mathrm{F}}^2 \frac{d^2}{dp_{\mathrm{F}}^2}\left(\frac{\epsilon}{n}\right) = 250 \text{ MeV} \tag{11.35}$$

Of these, the compressibility has the greatest uncertainty, approximately ± 30 MeV. With the freedom of two additional parameters, b and c, in the Lagrangian it is possible to fit all four of the above numbers.

The consequences of adding the cubic and quartic terms are to add to the energy density the quantity $\frac{1}{3}bm_N(g_\sigma\bar{\sigma})^3 + \frac{1}{4}c(g_\sigma\bar{\sigma})^4$ and to subtract
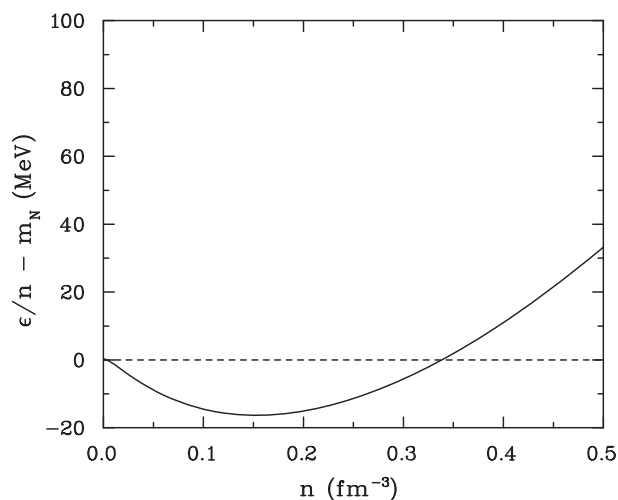
Fig. 11.6. The average energy per nucleon minus the nucleon mass as a function of baryon density in the mean field approximation when three- and four-body forces are included.

the same amount from the pressure. The self-consistency condition for the mean scalar field that replaces (11.14) is

$$m_\sigma^2 \bar\sigma + b m_N g_\sigma^3 \bar\sigma^2 + c g_\sigma^4 \bar\sigma^3 = g_\sigma n_s \qquad (11.36)$$

where once again n_s is the scalar density. One deduces from a numerical calculation that $g_\sigma^2/4\pi = 6.003$, $g_\omega^2/4\pi = 5.948$, $b = 7.950 \times 10^{-3}$, and $c = 6.952 \times 10^{-4}$. The resulting equation of state is plotted in Figure 11.6. This may be viewed as a means of quantifying the nuclear equation of state in such a way that known nuclear properties are fitted at saturation density and also that the extrapolation to both lower and higher densities is consistent with the principles of relativity and is thermodynamically consistent.

11.4 Liquid–gas phase transition

It is generally true that any system of fermions that is self-bound, in three space dimensions, will undergo a liquid–gas phase transition. This phase transition is essentially of the Van der Waals type. The reason for a phase transition is easy to understand intuitively. First, consider nuclear matter at $T = 0$ and density $n < n_0$. The binding energy curves of Figures 11.2 and 11.6 suggest that it is energetically favorable for the nucleons to form isolated clumps or droplets with a local density n_0 rather than to be distributed homogeneously throughout space. The space surrounding

the isolated droplets is simply a vacuum. As the temperature is turned up from zero, two things happen. Nucleons within a droplet have an increased kinetic energy owing to the finite temperature, and so the droplet swells in size and is reduced in local density. Finite temperature also means that the droplets will evaporate nucleons into what was formerly the vacuum. Thus we have a phase mixture: isolated droplets of nuclear liquid with local density $n_L < n_0$ are surrounded by a nuclear gas with density $n_G < n_L$. As T increases, n_G increases and n_L decreases. Eventually, at some temperature T_c we reach a critical point where $n_G = n_L$ and the distinction between liquid and gas disappears.

The liquid–gas phase transition is readily studied in the relativistic mean field model of nuclear matter with cubic and quartic interactions. The equation of state is

$$P(\mu, T) = P_{FG} + \tfrac{1}{2}\left(\frac{g_\omega^2}{m_\omega^2}\right)n^2 - \tfrac{1}{2}m_\sigma^2\bar{\sigma}^2 - \tfrac{1}{3}bm_N(g_\sigma\sigma)^3 - \tfrac{1}{4}cm_N(g_\sigma\sigma)^4$$

(11.37)

where

$$P_{FG} = 4T\int\frac{d^3p}{(2\pi)^3}\left[\ln\left(1 + e^{-\beta(E^*-\mu^*)}\right) + \ln\left(1 + e^{-\beta(E^*+\mu^*)}\right)\right]$$

$$n = 4\int\frac{d^3p}{(2\pi)^3}\left(\frac{1}{e^{\beta(E^*-\mu^*)}+1} - \frac{1}{e^{\beta(E^*+\mu^*)}+1}\right)$$

$$n_s = 4\int\frac{d^3p}{(2\pi)^3}\frac{m_N^*}{E^*}\left(\frac{1}{e^{\beta(E^*-\mu^*)}+1} + \frac{1}{e^{\beta(E^*+\mu^*)}+1}\right)$$

$$E^* = \sqrt{p^2 + m_N^{*2}}$$

$$g_\sigma n_s = m_\sigma^2\bar{\sigma} + bm_N g_\sigma^3\bar{\sigma}^2 + cg_\sigma^4\bar{\sigma}^3$$

$$m_N^* = m_N - g_\sigma\bar{\sigma}$$

$$\mu^* = \mu - \left(\frac{g_\omega^2}{m_\omega^2}\right)n$$

(11.38)

From these it is possible to verify the thermodynamic identity $n = \partial P(\mu, T)/\partial\mu$, and to compute the entropy density and energy density according to $s = \partial P(\mu, T)/\partial T$, $\epsilon = -P + Ts + \mu n$. Strictly speaking, the contribution of thermal mesons should be added. However, for the temperatures of interest here, $T < 30$ MeV, the σ and ω mesons contribute very little since $T \ll m_\sigma, m_\omega$.

Some isotherms of pressure versus density are plotted in Figure 11.7. Consider moving along the $T = 10$ MeV isotherm. For very small n, $0 < n < n_A$, only the gas phase is present. When $n > n_D$, only the liquid
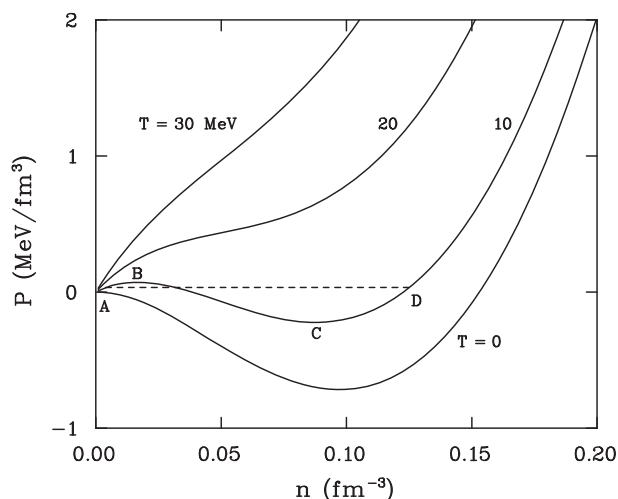
Fig. 11.7.   Isotherms of pressure versus baryon density in the mean field approximation with the inclusion of three- and four-body forces. The horizontal line is the Maxwell construction for phase equilibrium. The critical temperature is 16.4 MeV.

phase is present. The points A and D are defined by the condition that they have the same value of the chemical potential μ. The straight line connecting A and D is the Maxwell construction. For densities $n_A < n < n_D$ the equilibrium configuration is a mixture of the liquid phase (with local density n_D) and the gas phase (with local density n_A). The reason is that the Gibbs criterion of equal P, T, and μ is satisfied. From A to B it is possible for the system to remain in the gas phase, but it is metastable and will not survive indefinitely. Similarly the liquid phase is metastable from C to D. The portion of the curve between B and C is unstable. Recall the stability condition [21] $\partial P(n, T)/\partial n > 0$. If the inequality does not hold then the isothermal speed of sound is imaginary and isothermal perturbations will grow exponentially.

For $T < T_c$, the phase transition is first order. At T_c, the points A, B, C, D merge into one point, an inflection point, also called the critical point. At the critical point, the line of first-order phase transitions terminates in a second-order one. For $T > T_c$, there is no distinction between gas and liquid and no phase transition.

The critical temperature in this model is 16.4 MeV. Other models of nuclear matter typically yield T_c in the range 14–19 MeV [22–25]. Generally, T_c is a monotonically increasing function of the compressibility K.

There have been attempts, which have met with some success, to find experimental evidence of a nuclear liquid–gas phase transition in heavy ion collisions. Unlike in the theory, in the experiments the Coulomb force cannot be turned off and this complicates the analysis. Interested readers are referred to the reviews by Csernai and Kapusta [26] and by Das Gupta, Mekjian, and Tsang [27].

11.5 Summary

The relativistic field theories used to describe dense nuclear matter can only be effective because nucleons and mesons are composite objects, constructed in a complicated way from quark and gluon fields. Nevertheless, nucleons and mesons are the relevant degrees of freedom for densities up to perhaps four to eight times nuclear saturation density and temperatures less than about 150 MeV. One should not think of the effective Lagrangians as providing a fundamental theory that must be solved to all orders in the coupling constants. On the contrary, this is bound to fail because of the large numerical values of the coupling constants. Explicit two-loop calculations with point vertices show just how large these contributions can be. Inserting physically plausible form factors at the vertices softens these contributions considerably, resulting in only minor corrections to the relativistic mean field or relativistic Hartree approximations. The practical view, which we espouse, is that the relativistic mean field approximation is the simplest way to parametrize the nuclear equation of state. It does so in a way that embodies as much of our empirical knowledge as possible (binding energy and density, compressibility, etc.) while being consistent with special relativity and the thermodynamic identities. The approach is flexible enough to allow such additional degrees of freedom and additional interaction terms as are necessary to bring about agreement with new data on nuclear matter properties.

In this brief introduction to the subject of dense nuclear matter, we have focused on relatively simple, renormalizable, Lagrangians with only a vector meson and a scalar meson. Much work has been and continues to be done with theories involving more mesonic degrees of freedom, such as ρ mesons, pions, and kaons, and more baryonic degrees of freedom, such as hyperons and delta resonances. An extension of this sort is presented in Chapter 16 for the purpose of obtaining the equation of state to be used in computing the structure of neutron stars. Since these theories are effective-field theories there is no reason why they should be restricted to normalizable interactions. In principle, all low-lying degrees of freedom and all interactions consistent with the symmetries of QCD ought to be allowed. Such low-energy expansions have been worked out by Furnstahl,

Serot, and Tang [28]. Not only must the effective Lagrangian be consistent with the symmetries of QCD, so also must the approximations one employs to calculate the properties of nuclear matter. The problem of the pion self-energy in nuclear matter [29, 30] is a good illustration of how chiral symmetry can be violated by the mean field approximation when used in conjunction with certain representations of the pion–nucleon interaction.

11.6 Exercises

11.1 Evaluate the integrals that result in (11.17).

11.2 Calculate $\int d^3r\, V(r)$ using (11.3) and evaluate it numerically with the parameters of the Walecka model. Show that the nonrelativistic limit of the Walecka equation of state is equivalent to the sum of the average kinetic and potential energies calculated directly from the nonrelativistic Hamiltonian in the mean field approximation.

11.3 Verify the Hugenholtz–Van Hove theorem [31], which states that the single-particle energy at the Fermi surface equals the binding energy per nucleon at saturation density, for the Walecka model.

11.4 Derive the formula (11.31).

11.5 Calculate the nuclear optical potential with the inclusion of three- and four-body interactions. Compare the result with the cited literature on the optical potential used in proton–nucleus and nucleus–nucleus scattering experiments.

11.6 Estimate the dependence of the critical temperature and density of the nuclear liquid–gas phase transition on the binding energy, compressibility and other nuclear matter properties as follows. Near the saturation point of cold nuclear matter the energy per nucleon may be parametrized as

$$E_0(n) = \frac{K}{18}\left(\frac{n}{n_0} - 1\right)^2 - B$$

where $B = 16.3$ MeV is the binding energy. If the thermal excitation energy is taken to be that of a degenerate Fermi gas then the pressure may be written as

$$P(n,T) = \frac{K}{9}\frac{n^2}{n_0}\left(\frac{n}{n_0} - 1\right) + \frac{1}{3}\left(\frac{2\pi}{3}\right)^{2/3} mn^{1/3}T^2$$

See [32] for more details, especially regarding the entropy.

References

1. Johnson, M. H., and Teller, E., *Phys. Rev.* **98**, 783 (1955).
2. Duerr, H.-P., *Phys. Rev.* **103**, 469 (1956).
3. Walecka, J. D., *Ann. Phys. (NY)* **83**, 491 (1974).
4. Möller, P., Myers, W. D., Swiatecki, W. J., and Treiner, J., *At. Data Nucl. Data Tables* **39**, 225 (1988); Myers, W. D. and Swiatecki, W. J., *Phys. Rev. C* **57**, 3020 (1998).
5. Blaizot, J.-P., *Phys. Rep.* **64**, 171 (1980); Blaizot, J.-P., Berger, J. F., Decharge, J., and Girod, M., *Nucl. Phys.* **A591**, 435 (1991).
6. Khoa, Dao T., Satchler, G. R., and Von Oertzen, W., *Phys. Rev. C* **56**, 954 (1997).
7. Youngblood, D. H., Clark, H. L., and Lui, Y. W., *Phys. Rev. Lett.* **82**, 691 (1999).
8. Johnson, C. H., Horen, D. J., and Mahaux, C., *Phys. Rev. C* **36**, 2252 (1987).
9. Jaminon, M., and Mahaux, C., *Phys. Rev. C* **40**, 354 (1989).
10. Furnstahl, R. J., Rusnak, J. J., and Serot, B. D., *Nucl. Phys.* **A632**, 607 (1998).
11. Machleidt, R., Holinde, K., and Elstor, Ch., *Phys. Rep.* **149**, 1 (1987).
12. Serot, B. D., and Walecka, J. D., *Int. J. Mod. Phys. E* **6**, 515 (1997).
13. Arnold, L. G., *et al.*, *Phys. Rev. C* **25**, 936 (1982).
14. Gale, C., Bertsch, G., and Das Gupta, S., *Phys. Rev. C* **35**, 1666 (1987).
15. Aichelin, J., Rosenhauer, A., Peilert, G., Stöcker, H., and Greiner, W., *Phys. Rev. Lett.* **58**, 1926 (1987).
16. Chin, S. A., *Ann. Phys. (NY)* **108**, 301 (1977).
17. Furnstahl, R. J., Perry, R. J., and Serot, B. D., *Phys. Rev. C* **40**, 321 (1989).
18. Prakash, M., Ellis, P. J., and Kapusta, J. I., *Phys. Rev. C* **45**, 2518 (1992).
19. Sakurai, J. J. (1969). *Currents and Mesons* (University of Chicago Press).
20. Serot, B. D., and Tang, H.-B., *Phys. Rev. C* **51**, 969 (1995).
21. Landau L. D., and Lifshitz, E. M. (1959). *Statistical Physics* (Addison-Wesley).
22. Walecka, J. D., *Phys. Lett.* **B59**, 109 (1975); Freedman, R. A., *ibid.* **B71**, 369 (1977).
23. Sauer, G., Chandra, H., and Mosel, U., *Nucl. Phys.* **A264**, 221 (1976).
24. Lattimer, M., and Ravenhall, D. G., *Astrophys. J.* **223**, 314 (1978).
25. Friedman, B., and Pandharipande, V. R., *Nucl. Phys.* **A361**, 502 (1981).
26. Csernai, L. P., and Kapusta, J. I., *Phys. Rep.* **131**, 223 (1986).
27. Das Gupta, S., Mekjian, A. Z., and Tsang, M. B., *Adv. Nucl. Phys.* **26**, 89 (2001).
28. Furnstahl, R. J., Serot, B. D., and Tang, H.-B., *Nucl. Phys.* **A615**, 441 (1997); **A640**, 505 (E) (1998).
29. Kapusta, J. I., *Phys. Rev. C* **23**, 1648 (1981).
30. Matsui, T., and Serot, B. D., *Ann. Phys. (NY)* **144**, 107 (1982).
31. Van Hove, L., and Hugenholtz, N. M., *Physica* **24**, 363 (1958).
32. Kapusta, J. I., *Phys. Rev. C* **29**, 1735 (1984).

Bibliography

Relativistic nuclear field theories

Serot, B. D., and Walecka, J. D., *Adv. Nucl. Phys.* **16**, 1 (1986).

Serot, B. D., *Rep. Prog. Phys.* **55**, 1855 (1992).

Serot, B. D., and Walecka, J. D., *Int. J. Mod. Phys. E* **6**, 515 (1997).